Electron temperatures and electron densities in microwave helium discharges with pressures higher than 0.1 MPa

Koichi Sasaki[*1], **Shuntaro Soma**[1], **Haruaki Akashi**[2], **Mansour ElSabbagh**[3], and **Yuji Ikeda**[4]

[1] Division of Quantum Science and Engineering, Hokkaido University, Kita 13, Nishi 8, Kita-ku, Sapporo 060-8628, Japan

[2] Department of Applied Physics, National Defense Academy, 1-10-20 Hashirimizu, Yokosuka 239-8686, Japan

[3] Plasma and Laser Laboratory, Al-Azhar University, Nasr City, Cairo, Egypt

[4] Imagineering, Inc., 7-4-4 Minatojima-Minami, Chuo-ku, Kobe 650-0047, Japan

Key words electron temperature, electron density, multi-atmospheric-pressure plasma, Thomson scattering, plasma-assisted combustion

We adopted laser Thomson scattering for measuring the electron density and the electron temperature of microwave plasmas produced in helium at the pressures higher than the atmospheric pressure. The electron density decreased while we observed the increase in the electron temperature with the pressure. These are reasonable results by considering the decrease in the reduced electric field, the dominant loss of electrons via three-body recombination with helium as the third body, and the production electrons with medium energy via heavy particle collisions at the high gas pressure. The temporal variation of the electron temperature had the rise and the fall time constants of approximately 10 ns. The rapid heating and cooling of the electron temperature are due to the fast energy transfer from electrons to helium because of the high collision frequency in the high-pressure discharge.

1 Introduction

This work is motivated by the development of a system for the plasma-assisted combustion [1] in automobile engines. Technologies for realizing ultralean combustion of automobile engines are important to reduce the consumption of fossil fuels and to curb the global warming. The most difficult point in the ultralean combustion is the ignition. A widely-used method of igniting combustion reactions of petrol engines is to produce a spark discharge using a so-called glow plug. However, the spark discharge obtained by using a commercial glow plug

* Corresponding author: e-mail: sasaki@qe.eng.hokudai.ac.jp, Phone: +81 11 706 6654, Fax: +81 11 706 6655

cannot ignite combustion reactions in a ultralean condition. Our attempt is to produce a plasma with a larger volume than the spark discharge to realize combustion in the ultralean condition.

The plasma-assisted combustion (or ignition) of a petrol engine needs a nonequilibrium plasma. This is because the increase in the gas temperature up to 4000 K results in the significant emission of NO_x [2]. The typical temperature of a thermal plasma is 10^4 K. The high temperature may improve the ignition property of the lean-fuel gas mixture, but we cannot use a thermal plasma for the plasma-assisted combustion because of the NO_x emission. Since the gas pressure inside petrol engines is higher than the atmospheric pressure, it is necessary to employ a method which can produce a nonequilibrium plasma even in a multi-atmospheric-pressure gas.

Ikeda *et al*. have developed a spark-plug assisted microwave plasma source with the intention of applying it to the plasma-assisted ignition in petrol engines [3, 4]. This plasma source works at multi-atmospheric pressures. Recently, atmospheric-pressure plasmas attract a great deal of attention from many researchers since they have various applications in the treatment of liquid media [5–8] and biological tissues [9, 10]. However, the investigations on plasmas with pressures higher than the atmospheric pressure is relatively rare. The objective of this work is to investigate the electron temperature and the electron density in the microwave plasma source. Since the plasma has a high pressure and a small volume, only a possibility to determine the plasma parameters is to use laser Thomson scattering. We constructed a system of laser Thomson scattering, and adopted it for measuring the electron density and the electron temperature in the microwave plasma source. We discuss the kinetics of charged species in the high-pressure plasma on the basis of experimental observations.

2 Experiment

The experimental apparatus is schematically shown in Fig. 1(a), and the details of the microwave plasma source are shown in Fig. 1(b). Figure 1(c) shows a picture of a microwave discharge. It is noted that the plasma source shown in Fig. 1(b) is a prototype and is not applicable to petrol engines in the present form. The discharge part was composed of two cylindrical electrodes 3 mm in diameter. The gap distance between the two electrodes was 12 mm. The two electrodes were installed in a cylindrical microwave cavity which was made of aluminum with an inner diameter of 75 mm and a height of 120 mm. The cavity had four 16 mm holes in diameter. The cavity and the electrodes were installed in a cylindrical stainless-steel chamber which was connected to an oil rotary pump. The chamber had four quartz windows which were resistant to a high pressure up to 1 MPa. After evacuating the chamber using an oil rotary pump, we introduced pure helium into the chamber. The gas was not flowing.

The upper electrode was connected to a microwave power supply with a coaxial cable. The power supply was a semiconductor-based microwave generator at a frequency of approximately 2.45 GHz. The frequency is tunable around 2.45 GHz, and the impedance matched to the efficient power transmission was obtained by tuning the microwave frequency. The microwave power was pulse modulated at a repetition frequency of 10 Hz. The

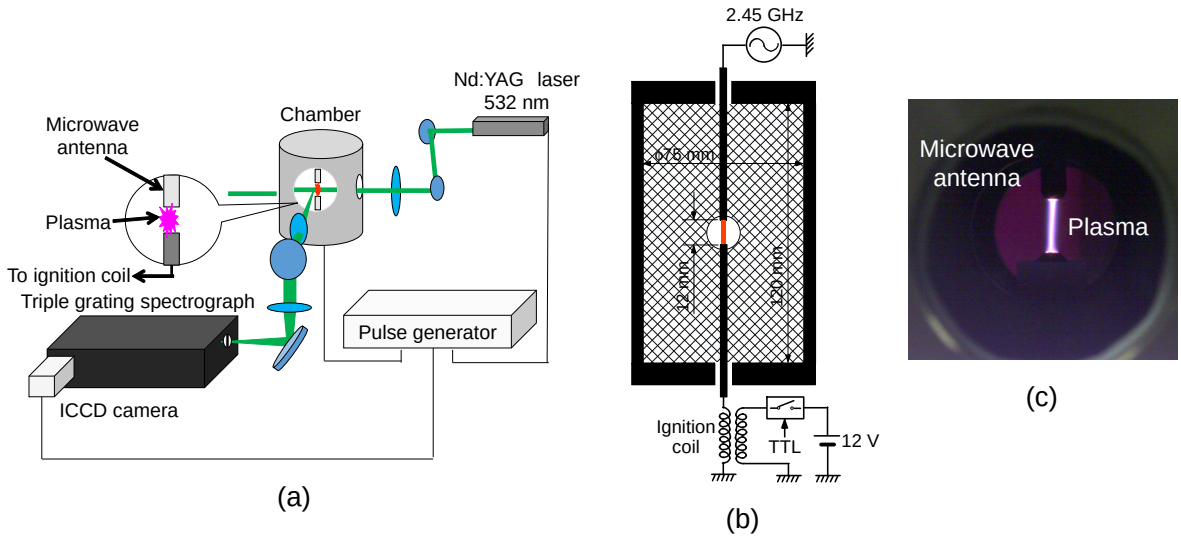

Fig. 1 Experimental apparatus: (a) schematic of the entire experimental system including the plasma source and the system of laser Thomson scattering, (b) details of the plasma source, and (c) picture of the microwave helium discharge.

duration and the instantaneous power of the microwave were 2 ms and 200 W, respectively. The microwave power had the rise and the fall time constants of approximately 20 ns, which were measured by picking up the microwave power using a directional coupler. The bottom electrode was connected to an ignition coil. The ignition coil was a commercial one which is widely used in petrol engines. The ignition coil supplied a high-voltage pulse to the bottom electrode to produce a spark discharge at the timing of the TTL trigger. The spark discharge was necessary to ignite a microwave plasma. The pulsed microwave power was initiated at 0.5 ms after the spark discharge. After the ignition, the plasma was sustained by the microwave power.

Nd:YAG laser pulses at a wavelength of 532 nm was injected into the gap between the two electrodes via the window on the chamber and the hole on the cavity at various delay times after the initiation of the pulsed microwave power. A lens was used for focusing the laser beam. It was necessary to attenuate the energy of the YAG laser pulse below 7 mJ/pulse to avoid the disturbance to the plasma. The scattered laser light was collected using a lens and was projected onto the entrance slit of a triple-grating spectrograph [11, 12] with a focal length of 200 mm. The triple-grating spectrograph was equipped with three diffractive gratings (1800 grooves/mm), an intermediate slit, a Rayleigh block, and an ICCD camera. The Rayleigh block was an important component to eliminate the stray light and the Rayleigh scattered light efficiently. The ICCD camera worked at the photon counting mode. We recorded four signals to obtain the Thomson scattering spectrum. The first one ($I_{\mathrm{P+L}}$) was the signal obtained with the presences of both the plasma and the YAG laser beam. The second signal (I_{P}) was obtained with the presence of the plasma only by which we observed the optical emission spectrum of the plasma. The third signal (I_{L}) was obtained with the presence of the laser beam only by which we observed the residual stray light. The last signal (I_{D}) was the dark level which was observed in the absence of both the

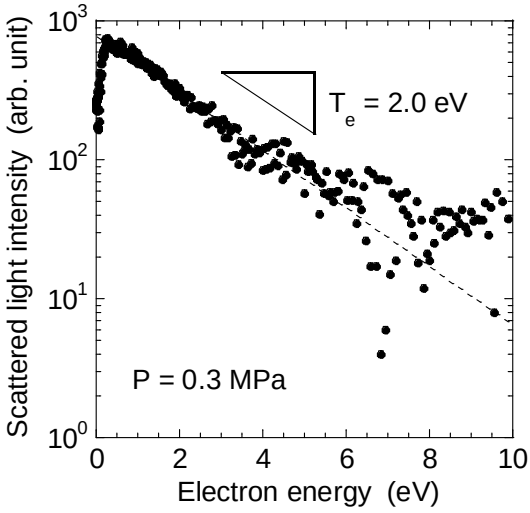

Fig. 2 Typical electron energy distribution function measured by laser Thomson scattering in a microwave helium plasma at a pressure of 0.3 MPa.

plasma and the laser beam. The Thomson scattering spectrum was calculated by $I_{\mathrm{P+L}} - I_{\mathrm{P}} - I_{\mathrm{L}} + I_{\mathrm{D}}$. The signals were accumulated for 36000 laser shots to improve the signal-to-noise ratio. The electron temperature was obtained from the Thomson scattering spectrum directly. To evaluate the electron density, we replaced helium inside the chamber with nitrogen gas, and detected rotational Raman scattering of molecular nitrogen at a certain pressure [13]. The absolute electron density was determined by the ratio between the intensities of Thomson and Raman scattered lights.

3 Results

Figure 2 shows a typical electron energy distribution function which was obtained from the Thomson scattering spectrum by converting the wavelength to the kinetic energy of electron. The helium pressure was 0.3 MPa. The dip in the scattered light intensity around the origin of the horizontal axis is due to the Rayleigh block which worked as a notch filter around the laser wavelength. The Thomson scattered light was observed in both the shorter and the longer wavelength sides than the laser wavelength, and the spectrum in both sides are plotted in Fig. 2. As shown in the figure, we obtained a sufficient signal-to-noise ratio in the range of the electron energy below 6 eV. The electron temperature of 2 eV was evaluated from the slope of the exponential curve shown in Fig. 2. Since the signal-to-noise ratio was insufficient in the range of electron energy above 7 eV, we are not sure about the existence of the high-energy tail component in the electron energy distribution function. The limited dynamic range of the measurement was caused by the limitation in the laser energy for avoiding the disturbance in the plasma, and it is difficult to apply this Thomson scattering measurement to a real fuel mixture.

Figure 3 shows the electron temperature and the electron density as a function of the helium pressure. They were measured at three delay times of 0.2, 1.0, and 1.9 ms after the initiation of the microwave power. The electron density decreased with the delay time as shown in Fig. 3(b), while we observed no trend in the temporal variation of the electron temperature. The details of the temporal variations of the electron temperature and

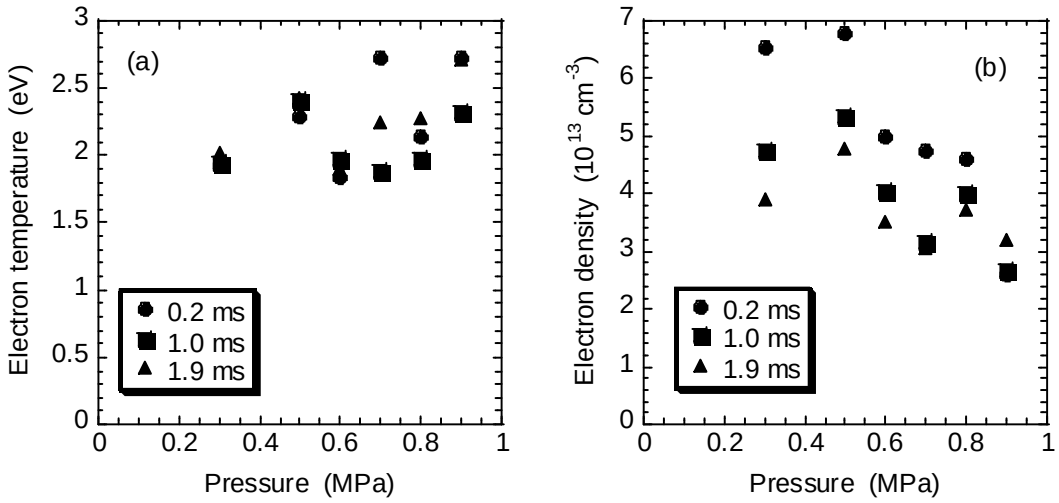

Fig. 3 Pressure dependences of (a) the electron density and (b) the electron temperature. Values observed at three delay times after the initiation of the microwave power are plotted.

the electron density will be described in the next paragraph. As shown in Fig. 3(b), the electron density in the microwave plasma was on the order of 10^{13} cm^{-3}. It was found that the electron temperature was higher than 1.5 eV at all discharge conditions as shown in Fig. 3(a). On the other hand, the gas temperatures of the same plasmas, which were evaluated from the optical emission spectrum of impurity OH ($\mathrm{X}^2\Pi(v''=0)-\mathrm{A}^2\Sigma^+(v'=0)$ transition), were lower than 3000 K. Therefore, it has been confirmed that this plasma source can produce nonequilibrium plasmas in helium. It should be emphasized here that the electron temperature increased with the pressure, while we observed the decrease in the electron density with the pressure.

The temporal evolutions of the electron temperature and the electron density after the initiation of the microwave power are shown in Fig. 4. The discharge pressure was 0.3 MPa. The vertical error bars indicate the ambiguities when evaluating the electron temperature and the electron density from the Thomson scattering spectrum. The horizontal error bars show the duration of the YAG laser pulse. As shown in Fig. 3(a), we observed an electron temperature of ~ 3 eV at 10 ns after the initiation of the microwave power. The electron temperature decreased with the time to ~ 10 μs. After that we observed a stationary electron temperature of ~ 2 eV. On the other hand, the electron density gradually increased in time, and the maximum electron density of 6.6×10^{13} cm^{-3} was observed at ~ 100 μs. After that we observed the temporal decrease in the electron density.

Figure 5 shows the temporal decays of the electron temperature and the electron density observed in the afterglow at a pressure of 0.3 MPa. We observed a rapid decay of the electron temperature in the initial afterglow as shown in Fig. 5(a). The decrease in the electron temperature after the rapid decay happened slowly, and the plasma kept an electron temperature of ~ 0.5 eV until 10 μs after the termination of the microwave power. The decay of the electron density was gradual as shown in Fig. 5(b).

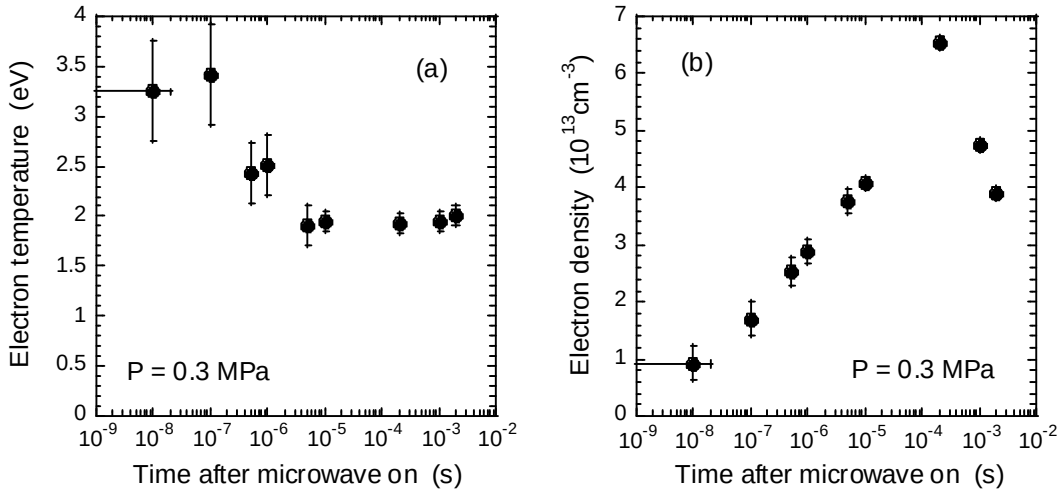

Fig. 4 Temporal evolutions of (a) the electron temperature and (b) the electron density after the initiation of the microwave power. The helium pressure was 0.3 MPa.

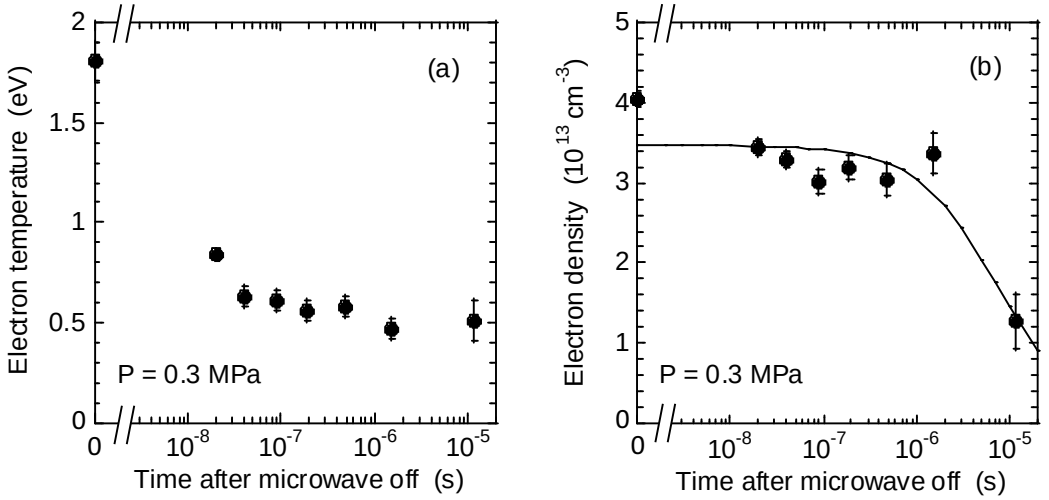

Fig. 5 Temporal decays of (a) the electron temperature and (b) the electron density after the termination of the microwave power. The helium pressure was 0.3 MPa.

4 Discussion

As shown in Fig. 3(b), we observed the decrease in the electron density with the pressure while the electron temperature increased with the pressure as shown in Fig. 3(a), even though the experimental data had considerable scattering. The cause of the data scattering has not been fully understood yet, however it might be attributed to the uncontrollable impurity concentrations in the chamber. The pressure dependences of the electron temperature and the electron density shown in Fig. 3 contradict the general understanding of the pressure dependence of the plasma parameters. However, they can be explained as follows, on the basis of the particle balance [**?**] of the plasma.

The production process of a pair of an electron and an ion is the electron impact ionization $\mathrm{He} + \mathrm{e} \rightarrow \mathrm{He}^+ + \mathrm{e} + \mathrm{e}$, and it is followed by a three-body reaction $\mathrm{He}^+ + \mathrm{He} + \mathrm{He} \rightarrow \mathrm{He}_2^+ + \mathrm{He}$. Therefore, it is certain that the dominant ion species in the high-pressure plasma is the dimer ion of helium (He_2^+). In addition, it is also certain that the ambipolar diffusion loss of He_2^+ is negligible in the high-pressure plasma, and the dominant loss process of the plasma is the volume recombination. A recombination process is dissociative recombination $\mathrm{He}_2^+ + \mathrm{e} \rightarrow \mathrm{He} + \mathrm{He}$. This reaction has a rate coefficient of 1×10^{-10} cm^3/s at an electron temperature of 0.5 eV (the electron temperature observed in the afterglow) [14]. Another recombination process is the three-body recombination, and we consider the following two species for the third body. The three-body recombination $\mathrm{He}_2^+ + \mathrm{e} + \mathrm{e} \rightarrow \mathrm{He} + \mathrm{He} + \mathrm{e}$ has a two-body rate coefficient of 1×10^{-11} cm^3/s at an electron temperature of 0.5 eV and an electron density of 3×10^{13} cm^{-3}, while $\mathrm{He}_2^+ + \mathrm{e} + \mathrm{He} \rightarrow \mathrm{He} + \mathrm{He} + \mathrm{He}$ has a two-body rate coefficient of 8×10^{-9} cm^3/s at an electron temperature of 0.5 eV, the gas temperature of 3000 K, and a gas pressure of 0.3 MPa [14]. According to the rate coefficients listed above, the dominant loss process of the plasma is believed to be the three-body recombination with helium as the third body ($\mathrm{He}_2^+ + \mathrm{e} + \mathrm{He} \rightarrow \mathrm{He} + \mathrm{He} + \mathrm{He}$).

When the dominant loss process of the plasma is the volume recombination, the temporal variation of the electron density in the afterglow is given by

$$\frac{1}{n_\mathrm{e}(t)} = \frac{1}{n_\mathrm{e0}} + k_\mathrm{r} t, \tag{1}$$

where n_e0 is the electron density at $t = 0$ and k_r is the rate coefficient of the recombination. The solid curve illustrated in Fig. 5(b) shows eq. (1) with $k_\mathrm{r} = 4 \times 10^{-9}$ cm^3/s and $n_\mathrm{e0} = 3.5 \times 10^{13}$ cm^{-3}. As shown in the figure, eq. (1) with $k_\mathrm{r} = 4 \times 10^{-9}$ cm^3/s explains the temporal variation of the electron density in the afterglow. The close agreement between $k_\mathrm{r} = 4 \times 10^{-9}$ cm^3/s and the two-body rate coefficient of $\mathrm{He}_2^+ + \mathrm{e} + \mathrm{He} \rightarrow \mathrm{He} + \mathrm{He} + \mathrm{He}$ confirms that the three-body recombination with helium as the third body is the dominant loss process of the plasma. It is noted that the two-body rate coefficient of this reaction is proportional to the density of helium or the gas pressure. Therefore, we can expect the decrease in the lifetime of the plasma with the gas pressure in the present experimental condition.

On the basis of the aforementioned kinetics of charged particles, the electron density is approximately determined by the balance between the electron impact ionization and the recombination, and is given by

$$n_\mathrm{e} = \frac{k_\mathrm{i}}{k_\mathrm{r}}, \tag{2}$$

where k_i is the rate coefficient of $\mathrm{He} + \mathrm{e} \rightarrow \mathrm{He}^+ + \mathrm{e} + \mathrm{e}$. We can expect the decrease in k_i with the gas pressure because of the decrease in the reduced electric field. This may be the mechanism of Fig. 3(b) which shows the decrease in the electron density with the gas pressure. On the other hand, more complicated kinetics are necessary to explain the experimental result shown in Fig. 3(a). The first possible mechanism for the increase in the electron temperature with the gas pressure is the enhanced loss of low-energy electrons due to the recombination, since the recombination has a large cross section at a low electron energy. The loss of low-energy electrons means the increase in the mean electron energy, resulting in the higher electron temperature in the Thomson scattering

measurement. It is noted that this does not mean the increase in k_{i}. The increase in the mean electron energy is due to the loss of low-energy electrons and is not due to the production of high-energy electrons. The second possibility is the collision of two excimers $\mathrm{He}_2^* + \mathrm{He}_2^* \rightarrow \mathrm{He}_2^+ + \mathrm{e} + \mathrm{He} + \mathrm{He}$, which produces electrons with medium energy [15]. Since the high gas pressure enhances the excimer density, the rate of this reaction may be higher at a higher gas pressure. In addition, the third possibility is the production of electrons with medium energy via $\mathrm{He}^{\mathrm{M}} + \mathrm{He}^{\mathrm{M}} \rightarrow \mathrm{He}^+ + \mathrm{e} + \mathrm{He}$ [16, 17]. The rate of this reaction may become higher at a higher gas pressure because of the higher density of the metastable state (He^{M}). It is noted that the energy of electrons produced via $\mathrm{He}_2^* + \mathrm{He}_2^* \rightarrow \mathrm{He}_2^+ + \mathrm{e} + \mathrm{He} + \mathrm{He}$ and $\mathrm{He}^{\mathrm{M}} + \mathrm{He}^{\mathrm{M}} \rightarrow \mathrm{He}^+ + \mathrm{e} + \mathrm{He}$ is lower than the ionization potential of helium. Hence, these reactions may enrich the amount of electrons with medium energy, but it does not contribute to the increase in k_{i}. The enrichment of electrons with medium energy may result in the increase in the electron temperature with the gas pressure. Since the experimental results shown in Fig. 3 are thus explained, they suggest no need to pay attention to the transition to an equilibrium plasma at a pressure higher than 1 MPa. We can expect the nonequilibrium plasma-assisted combustion in practical petrol engines.

The temporal variations of the electron temperature shown in Figs. 4(a) and 5(a) indicate rapid heating and cooling of electrons in this plasma source. The rise and fall time constants of the electron temperature are approximately 10 ns. If we presume a cross section of 2×10^{-15} cm^2 for elastic collision between helium and electron with energies of 1-3 eV [18], the frequency of elastic collision in helium at a pressure of 0.3 MPa amounts to $\sim 10^{12}$ s^{-1}. Here we presumed a temperature of 3000 K for helium. Therefore the time constant of ~ 10 ns is acceptable as the confinement time of electron energy in this experimental condition, and the rise and fall time constants observed experimentally are explained by the energy transport from electrons to helium. Since the energy confinement time of neutral atoms in this plasma source is ~ 50 ms [19], the gas temperature is maintained at ~ 3000 K in the observation period in the afterglow. Therefore, the mostly-constant electron temperature observed at $t \geq 0.1$ μs after the termination of the microwave power is attributed to the equilibrium between the electron temperature and the gas temperature.

The gradual increase in the electron density shown in Fig. 4(b) may be due to the particle confinement time determined by $\mathrm{He}_2^+ + \mathrm{e} + \mathrm{He} \rightarrow \mathrm{He} + \mathrm{He} + \mathrm{He}$. The gradual increase in the electron density results in the production of a larger amount of low-energy electrons by electron impact ionization. This is a mechanism for the decrease in the electron temperature after the maximum at 0.1 μs after the initiation of the discharge. On the other hand, the mechanism of the decrease in the electron density after ~ 100 μs has not yet been explained. One possibility is the increase in the recombination rate, which is caused by the decrease in the electron temperature. However, according to Fig. 3, the decrease in the electron temperature stops at ~ 10 μs while the decrease in the electron density starts at ~ 100 μs.

5 Conclusions

We examined the electron temperature and the electron density in multi-atmospheric-pressure microwave helium plasmas. It has been confirmed that the plasma keeps the nonequilibrium state even at a high pressure up to 1 MPa. We observed ultrafast heating and cooling of the electron temperature which are explained by frequent elastic collision between electron and helium. The most important understanding obtained through this work is the increase in the electron temperature with the discharge pressure, which can be explained by the dominant loss of electrons via three-body recombination with helium as the third body and the production of electrons with medium energy via heavy particle collisions at the high gas pressure.

Acknowledgements This work was supported by the New Energy and Industrial Technology Development Organization (NEDO); Strategic Development of Energy Conservation Technology/Demonstration Research Phase. This work was also partly supported by JSPS KAKENHI Grant Number 25249015.

References

[1] S. M. Starikovskala, J. Phys. D **39**, R265 (2006).

[2] A. G. Gaydon and H. G. Wolfhand, *Flames, their structure, radiation and temperature, 4th ed.* (Chapman and Hall, London, 1979).

[3] Y. Ikeda, A. Nishiyama, Y. Wachi, and M. Kaneko, SAE International, Paper Number 2009-01-1050 (2009).

[4] Y. Ikeda, A. Nishiyama, H. Katano, M. Kaneko, and Jeong Han, SAE International, Paper Number 2009-01-1049 (2009).

[5] B. R. Locke, M. Sato, P. Sunka, M. R. Hoffmann, and J. S. Chang, Ind. Eng. Chem. Res. **45**, 882 (2006).

[6] B. Sun, M. Sato, A. Harano, and J. S. Clements, J. Electrostatics **43**, 115 (1998).

[7] M. Laroussi, IEEE Trans. Plasma Sci. **24**, 1188 (1996).

[8] S. Ikawa, K. Kitano, and S. Hamaguchi, Plasma Processes Polym. **7**, 33 (2010).

[9] G. Fridman, G. Friedman, A. Gutsol, A. B. Shekhter, V. N. Vasilets, and A. Fridman, Plasma Processes Polym. **5**, 503 (2008).

[10] M. G. Kong, G. Kroesen, G. Morfill, T. Nosenko, T. Shimizu, J. van Dijk, and J. L. Zimmermann, New J. Phys. **11**, (2009) 115012.

[11] K. Muraoka and A. Kono, J. Phys. D **44**, 043001 (2011).

[12] A. Kono and K. Nakatani, Rev. Sci. Instrum. **71**, 2761 (2000).

[13] A. F. H. van Gessel, E. A. D. Carbone, P. J. Bruggeman, and J. J. A. M. van der Mullen, Plasma Sources Sci. Technol. **21**, 015003 (2012).

[14] R. Deloche, P. Monchicourt, M. Cheret, and F. Lambert, Phys. Rev. A **13**, 1140 (1976).

[15] D. C. Lorents, Physica **82C**, 19 (1976).

[16] X. Yuan and L. L. Raja, IEEE Trans. Plasma Sci. **31**, 495 (2003).

[17] S. Rauf and M. J. Kushner, J. Appl. Phys. **85**, 3460 (1999).

[18] R. W. LaBahn and J. Callaway, Phys. Rev. A **2**, 366 (1970).

[19] M. ElSabbagh, S. Kado, Y. Ikeda, and K. Sasaki, Jpn. J. Appl. Phys. **50**, 076101 (2011).